



UNIVERSITY OF LEEDS

This is a repository copy of *On the Role of Radiative Processes in Stratosphere-Troposphere Coupling*.

White Rose Research Online URL for this paper:
<http://eprints.whiterose.ac.uk/43308/>

Article:

Grise, KM, Thompson, DWJ and Forster, PM (2009) On the Role of Radiative Processes in Stratosphere-Troposphere Coupling. *Journal of Climate*, 22 (15). 4154 - 4161 . ISSN 0894-8755

<https://doi.org/10.1175/2009JCLI2756.1>

Reuse

See Attached

Takedown

If you consider content in White Rose Research Online to be in breach of UK law, please notify us by emailing eprints@whiterose.ac.uk including the URL of the record and the reason for the withdrawal request.



eprints@whiterose.ac.uk
<https://eprints.whiterose.ac.uk/>

On the Role of Radiative Processes in Stratosphere–Troposphere Coupling

KEVIN M. GRISE AND DAVID W. J. THOMPSON

Department of Atmospheric Science, Colorado State University, Fort Collins, Colorado

PIERS M. FORSTER

School of Earth and Environment, University of Leeds, Leeds, United Kingdom

(Manuscript received 30 July 2008, in final form 24 February 2009)

ABSTRACT

Climate change in the Southern Hemisphere (SH) polar stratosphere is associated with substantial changes in the atmospheric circulation that extend to the earth's surface. The mechanisms that drive the changes in the SH troposphere are not fully understood, but most previous hypotheses have focused on the role of atmospheric dynamics rather than that of radiation.

This study quantifies the radiative response of temperatures in the SH polar troposphere to the forcing from long-term temperature and ozone trends in the SH polar stratosphere. A novel methodology is employed that explicitly neglects changes in tropospheric dynamics and hence isolates the component of the tropospheric temperature response that is radiatively driven by the overlying stratospheric trends. The results reveal that both the amplitude and seasonality of the observed cooling of the middle and upper SH polar troposphere over the past few decades are consistent with a reduction in downwelling longwave radiation induced by cooling in the SH polar stratosphere. The results are compared with analogous calculations for trends in the Northern Hemisphere (NH) polar stratosphere. Both the observations and radiative calculations imply that the comparatively weak trends in the NH polar stratosphere have not played a central role in driving NH tropospheric climate change.

Overall, the results suggest that radiative processes play a key role in coupling the large trends in SH polar stratospheric temperatures to tropospheric levels. The tropospheric radiative temperature response documented here could be important for triggering the changes in internal tropospheric dynamics associated with stratosphere–troposphere coupling.

1. Introduction

Observations and numerical simulations both suggest that variability in the extratropical stratosphere has a demonstrable impact on the extratropical troposphere. The coupling between stratospheric and tropospheric flow is observed in the context of Northern Hemisphere (NH) sudden stratospheric warmings (Baldwin and Dunkerton 1999, 2001; Limpasuvan et al. 2004), Southern Hemisphere (SH) sudden stratospheric warmings (Thompson et al. 2005), and recent trends in the SH polar regions (Thompson and Solomon 2002). The coupling is also evident in simulations run with rela-

tively simple general circulation models (e.g., Polvani and Kushner 2002) and in climate model responses to imposed SH polar stratospheric ozone depletion (e.g., Gillett and Thompson 2003; Arblaster and Meehl 2006).

For both the observed and simulated coupling, the tropospheric response includes substantial changes in the meridional flux of zonal momentum by the eddies near the tropopause (Limpasuvan et al. 2004; Kushner and Polvani 2004). For example, when the stratospheric flow is anomalously westerly, the poleward eddy momentum fluxes near the tropopause are enhanced across $\sim 45^\circ$ latitude, and thus the tropospheric zonal-mean zonal wind is anomalously westerly along 55° – 60° latitude but anomalously easterly along 35° – 40° latitude. The resulting tropospheric anomalies strongly resemble those associated with the positive polarity of the tropospheric annular mode (Baldwin and Dunkerton 2001).

Corresponding author address: Kevin M. Grise, Dept. of Atmospheric Science, Colorado State University, 1371 Campus Delivery, Fort Collins, CO 80523.
E-mail: kgrise@atmos.colostate.edu

Despite the robustness of stratosphere–troposphere coupling in observations and numerical simulations, there is still no consensus as to how the stratosphere triggers dynamical changes in the troposphere. The amplitude of the tropospheric wind response is consistent with the zonally symmetric “downward control” (e.g., Haynes et al. 1991) of the troposphere by anomalous stratospheric wave driving (Thompson et al. 2006). However, the downward control response does not explain the attendant changes in tropospheric eddy fluxes. Song and Robinson (2004) and Kushner and Polvani (2004) argue that the changes in tropospheric eddy fluxes are initiated by the downward control response in the troposphere. Alternatively, Wittman et al. (2007) and Chen et al. (2007) hypothesize that the changes in tropospheric eddy fluxes are driven directly by the lower-stratospheric zonal flow via its impact on the phase speed of the eddies and hence the latitude of subtropical wave breaking.

The aforementioned mechanisms are strictly dynamical, yet it is also plausible that the changes in tropospheric dynamics are triggered by the radiative heating of the troposphere by the overlying stratospheric anomalies. For example, climate change in the SH polar stratosphere is characterized by temperature and ozone anomalies that, to some extent, must perturb the radiative heating rates in the troposphere. Stratospheric ozone changes possess their strongest radiative influence on surface temperatures when they occur at or near the tropopause (e.g., Forster and Shine 1997). The radiative forcing arises from the reduction in downwelling longwave radiation caused by the cooling associated with ozone depletion in the lower stratosphere; in the Antarctic lower stratosphere, recent ozone-induced cooling has approached 8 K decade^{-1} (Randel and Wu 1999). Sudden stratospheric warmings are also characterized by large lower-stratospheric temperature changes (upward of $\sim 50 \text{ K}$; e.g., Reed et al. 1963), and the resulting changes in downwelling longwave radiation from the stratosphere have been theorized to reduce the available potential energy accessible to tropospheric eddy activity (Ramanathan 1977). However, to our knowledge, no study has explicitly quantified the importance of radiative processes for understanding recent observations of stratosphere–troposphere coupling.

The purpose of this paper is to quantify the importance of radiative processes in driving the polar tropospheric temperature anomalies observed in association with SH polar stratospheric climate trends. For comparison, we also investigate the tropospheric radiative temperature response to comparatively weak NH polar stratospheric climate trends. We focus solely on the role of radiative processes in stratosphere–troposphere coupling and hence neglect the impact of internal tro-

pospheric dynamics. Additionally, we do not examine the role of radiative processes in the stratosphere–troposphere coupling associated with individual sudden stratospheric warmings, since such events occur on time scales shorter than the radiative adjustment time scales of the lower stratosphere and upper troposphere. In section 2, we describe the observational datasets and statistical methods; in section 3, we review the observed temperature and ozone changes associated with the climate trends; and in section 4, we outline the experimental design and the numerical model used to estimate the tropospheric radiative temperature response. The results of the calculations are presented in section 5, and conclusions are provided in section 6.

2. Data and statistical methods

The temperature data used in this study are from the National Centers for Environmental Prediction–National Center for Atmospheric Research (NCEP–NCAR) reanalysis dataset (Kalnay et al. 1996) obtained from the Physical Sciences Division of the National Oceanic and Atmospheric Administration Earth System Research Laboratory. The data are restricted to the period following 1979 when the reanalysis data assimilation scheme includes more comprehensive satellite measurements (Kalnay et al. 1996; Kistler et al. 2001). As noted in section 3, the analyses based upon NCEP–NCAR reanalysis temperature data are consistent with those derived from radiosonde data.

Observations of polar stratospheric ozone are based on the Resolute ($\sim 75^\circ\text{N}$) and Syowa (69°S) ozonesonde profiles, which are available via the Canadian Ozone and Ultraviolet Measurement Program and the Japan Meteorological Agency Ozone Layer Monitoring Office, respectively. The ozonesonde data are used in the form provided by Randel and Wu (2007), in which 1979–2005 ozone anomaly time series have been fitted to the time series of equivalent effective stratospheric chlorine (EESC). The conclusions reached in our study are insensitive to the choice of using the raw ozonesonde data or the interpolated version provided by Randel and Wu (2007).

Long-term trends are approximated using composite differences between the 5-yr periods 1979–83 and 1997–2001. The former period corresponds to the first five years of data used in this study; the latter period corresponds to the latest contiguous 5-yr period of data that does not include the 2002 SH sudden stratospheric warming, the only observed major sudden stratospheric warming in the SH. In all cases, the composite differences are comparable to linear trends calculated over the period 1979–2001.

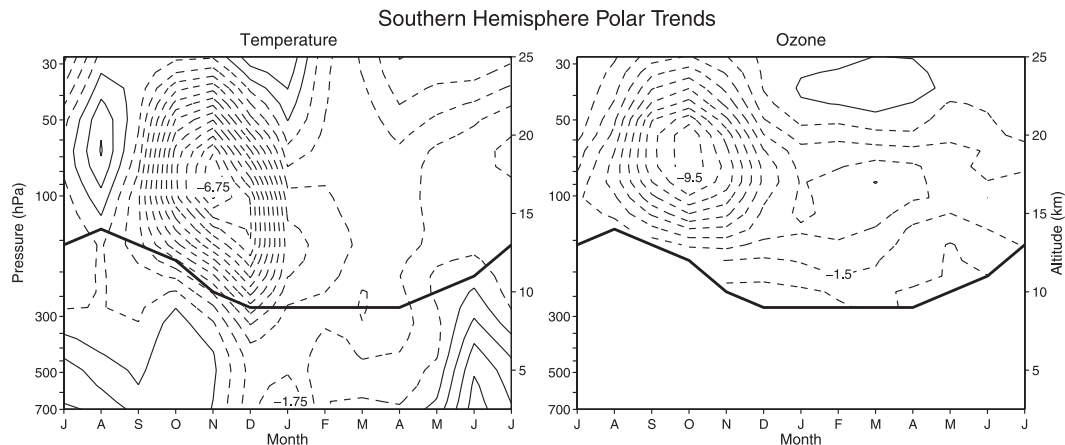


FIG. 1. The differences between the periods 1997–2001 and 1979–83 for (left) the NCEP–NCAR reanalysis temperatures averaged over 65° – 90° S and (right) Randel and Wu (2007) stratospheric ozone averaged over 65° – 90° S. Positive contours are solid, and negative contours are dashed. The contour intervals are (left) 0.5 K ($-0.75, -0.25, 0.25, 0.75, \dots$) and (right) 1 DU km^{-1} ($-1.5, -0.5, 0.5, 1.5, \dots$). The region above the solid black line is used to set the stratospheric conditions for the radiative calculations. Regions below 700 hPa are omitted because of the high altitude of the Antarctic continent.

3. Observational analysis

In this section, we review the polar temperature and ozone signals associated with long-term trends in the SH and NH polar stratospheres. The stratospheric components of the following results are used as input for the radiative calculations described in section 4. Because the tropospheric radiative temperature response does not depend upon the statistical significance of the long-term trends, we choose not to include a discussion of statistical significance here. The statistical significance of the long-term temperature trends has been previously documented by Thompson and Solomon (2002, 2005).

Figure 1 illustrates the differences in the SH polar (65° – 90° S) temperatures (left) and Syowa ozone (right) be-

tween the 5-yr periods 1979–83 and 1997–2001, and Fig. 2 illustrates the differences in the NH polar (60° – 90° N) temperatures (left) and Resolute ozone (right) between the same two 5-yr periods. The results are comparable to linear trends calculated over similar periods using radiosonde data (e.g., Thompson and Solomon 2002, 2005). In both Figs. 1 and 2, the solid black line denotes the seasonally varying height of the tropopause.

As noted in numerous previous studies (e.g., Solomon et al. 2005; see also Newman et al. 2007 and references therein), the largest ozone depletion in the SH polar stratosphere is observed during austral spring in association with the Antarctic ozone hole (Fig. 1, right). The peak polar ozone losses occur near 70 hPa between September and November, with weaker ozone losses

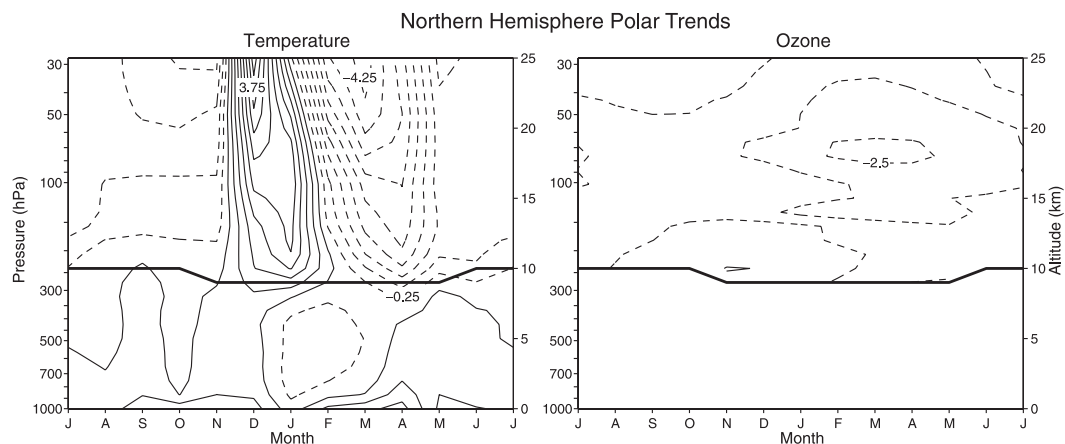


FIG. 2. As in Fig. 1, but for (left) 60° – 90° N and (right) 65° – 90° N. The lower bound for Fig. 2 is 1000 hPa.

present in the lower stratosphere throughout the year. The NH ozone losses are much weaker than their SH counterparts (Solomon et al. 2007) and peak near 70 hPa between February and April (Fig. 2, right).

In the SH polar stratosphere, the largest temperature decreases are observed during austral spring (Fig. 1, left; e.g., Randel and Wu 1999; Randel et al. 2009). The differences in the SH polar lower-stratospheric temperatures between the 1979–83 and 1997–2001 periods exceed 5 K in November and December and are consistent with the local radiative impact of the Antarctic ozone hole (Shine et al. 2003). The largest springtime cooling appears to descend below the tropopause during the months of December and January, in agreement with the trends in the tropospheric circulation observed at that time (Thompson and Solomon 2002).

The largest temperature decreases in the NH polar stratosphere also occur during spring (Fig. 2, left), but they are considerably smaller than those found in the SH (particularly below 100 hPa) and are accompanied by sizeable temperature increases during December and January. The stratospheric warming during December and January is consistent with increased wave-driven variability during early boreal winter (e.g., Randel et al. 2002; Manney et al. 2005). The deep stratospheric cooling during late boreal winter and early boreal spring is due in part to the local radiative impacts of the comparatively weak NH stratospheric ozone depletion (Fig. 2, right; Shine et al. 2003) but is also associated with decreases in planetary wave driving (e.g., Langematz et al. 2003; Newman et al. 2003). As noted in Thompson and Solomon (2005), the NH trends do not appear to descend below the tropopause level in a manner consistent with the SH trends.

In the following sections, we investigate the radiative influence of the stratospheric temperature and ozone changes shown in Figs. 1 and 2 on tropospheric temperatures. Section 4 details the radiative calculations, and the results of the calculations are given in section 5.

4. Radiative calculations

The radiative influence of the stratospheric temperature and ozone changes depicted in Figs. 1 and 2 on the troposphere is divided into two components: the temperature and emissivity/transmissivity effects. The temperature effect isolates the impact of anomalous longwave radiation associated with changes in stratospheric temperatures. The emissivity/transmissivity effect isolates the contribution of stratospheric ozone anomalies to changes in (i) the longwave emissivity at stratospheric levels and (ii) the transmission of shortwave radiation through the stratosphere.

The radiative calculations are performed using the Reading narrowband model (NBM) (e.g., Forster and Shine 1997; Forster and Shine 2002). The calculations isolate the radiatively induced temperature changes in the troposphere and, by design, neglect the effects of atmospheric eddy heat transport, the response of the surface, and convective adjustment. The importance of the latter processes is deferred to a future study, but for now can be interpreted as residing in the differences between the calculated radiatively induced temperature responses and the observed tropospheric temperature responses.

Following the methodology described in Forster et al. (1997), we divide the tendency in temperature at a given tropospheric level into radiative and dynamical components as follows:

$$\frac{dT}{dt} = Q_{\text{dyn}}(t) + Q_{\text{rad}}(t), \quad (1)$$

where $Q_{\text{rad}}(t)$ is the radiative heating rate and $Q_{\text{dyn}}(t)$ is the dynamical heating rate, which is assumed fixed to its climatological mean state such that

$$Q_{\text{dyn}}(t) \approx Q_{\text{dyn}}^C(t) = \frac{dT^C}{dt} - Q_{\text{rad}}^C(t), \quad (2)$$

where the terms on the right-hand side of (2) are computed from climatology. We determine $Q_{\text{dyn}}^C(t)$ by assuming that, within the time resolution of the analysis, (2) simplifies to $Q_{\text{dyn}}^C(t) = -Q_{\text{rad}}^C(t)$. In all cases, the time resolution of the analysis is one month, and the incident solar radiation is set to seasonally varying midmonthly values. Note that, since we wish to isolate the importance of radiative processes, the dynamical heating term $Q_{\text{dyn}}(t)$ in (1) is held fixed to climatological values $Q_{\text{dyn}}^C(t)$ in all calculations.

The tropospheric equilibrium temperature response for a given stratospheric temperature and ozone profile is calculated as follows: (i) the tropospheric radiative heating rates $Q_{\text{rad}}(t)$ in (1) are calculated for the prescribed stratospheric temperature and ozone values for a given month, and (ii) the temperatures in the free troposphere are adjusted until the net tropospheric heating rates $Q_{\text{rad}}(t)$ are equal and opposite to the climatological mean dynamical heating rate $Q_{\text{dyn}}^C(t)$ for that month (i.e., until the anomalous emission of radiation by the troposphere balances the stratospheric perturbation in radiation reaching the troposphere). Note that the methodology is analogous to the fixed dynamical heating assumption (e.g., Ramanathan and Dickinson 1979; Fels et al. 1980), except that the temperatures are adjusted in the troposphere rather than in the stratosphere.

Following the above procedure, the radiative effect of the trends in the SH polar (65° – 90° S) and NH polar (60° – 90° N) stratospheres on the polar troposphere is estimated in the following manner: (i) the tropospheric radiatively induced temperature response is calculated for SH and NH polar temperatures and ozone set to their seasonally varying 1979–83 average values above the tropopause (denoted by the solid black line in Figs. 1 and 2, respectively); (ii) the above procedure is repeated, but for temperatures and ozone set to their seasonally varying 1997–2001 average values above the tropopause; and (iii) the results in (i) are subtracted from those in (ii). In both cases, the temperatures and ozone below the tropopause and above 30 hPa are fixed initially to the radiation scheme's climatology (Forster and Shine 2002).

5. Results

a. Recent trends in the SH polar stratosphere

Results for trends in the SH polar stratosphere are shown in Fig. 3. The top panel is a reproduction of the observations from Fig. 1 (left); the middle panel depicts the temperature effect of the stratospheric anomalies; the bottom panel illustrates the sum of the temperature and emissivity/transmissivity effects of the stratospheric anomalies. Recall that, by construction, the observed and simulated changes are identical above the tropopause (solid black line).

The results in Fig. 3 highlight several key findings. First, both the amplitude and seasonality of the observed cooling in the mid- and upper troposphere are very similar to the radiative adjustment of the troposphere to reduced downwelling longwave radiation from the polar stratosphere. The correspondence is clearest between November and May when the observed temperature trends are largest.

Second, the radiative calculations do not account for the observed temperature trends in the lower troposphere. The discrepancies between the radiative calculations and the observed trends are clarified in Fig. 4, which shows differences between the top and bottom panels of Fig. 3. The differences in Fig. 4 may partially reflect artifacts in the NCEP–NCAR reanalysis (i.e., the surface height varies greatly over the SH polar cap), but they may also highlight the importance of vertical motion, meridional heat transport by the atmosphere, or radiative absorption at the surface, processes that are explicitly neglected by the calculations.

The third key result highlighted in Fig. 3 is that the net contribution of the emissivity/transmissivity effect is approximately zero, as evidenced by the near perfect

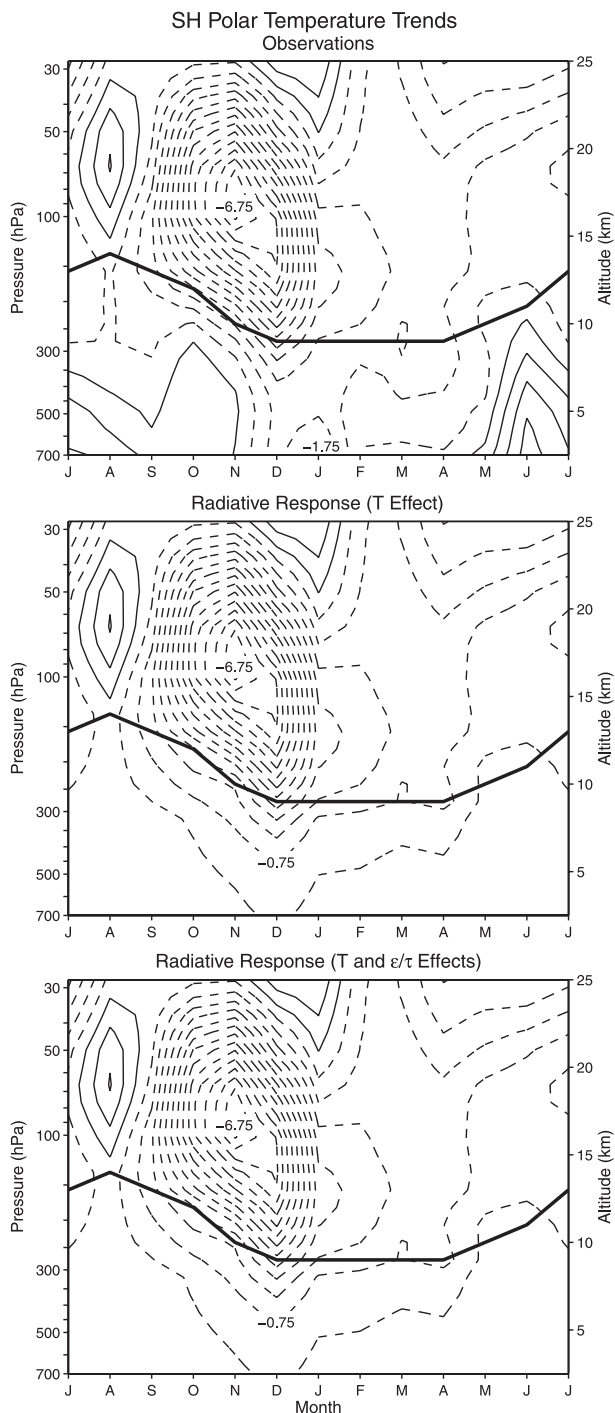


FIG. 3. (top) Reproduction of Fig. 1, left. (middle) The radiative temperature response to SH polar stratospheric temperature forcing (the temperature effect). (bottom) The radiative temperature response to SH polar stratospheric temperature and ozone forcings (the sum of the temperature and emissivity/transmissivity effects). Positive contours are solid, and negative contours are dashed. The contour interval is 0.5 K ($-0.75, -0.25, 0.25, 0.75, \dots$). The region above the solid black line is used to set the stratospheric conditions for the radiative calculations, and regions below 700 hPa are omitted because of the high altitude of the Antarctic continent.

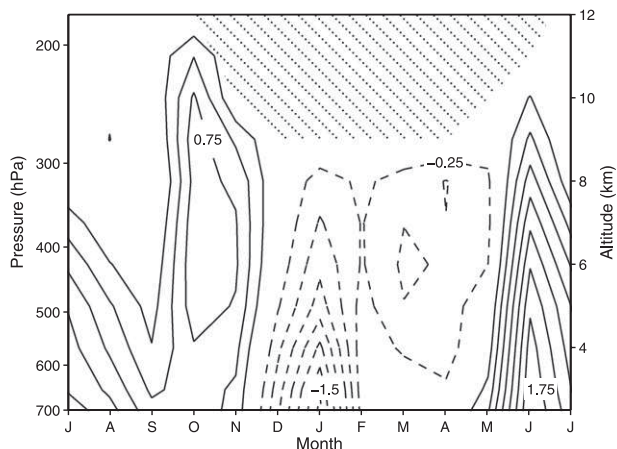


FIG. 4. Residual between top and bottom panels of Fig. 3. Positive contours are solid, negative contours are dashed, and the zero contour has been omitted. The contour interval is 0.25 K. Hatching indicates stratospheric levels. Regions below 700 hPa are omitted because of the high altitude of the Antarctic continent.

correspondence between the middle and bottom panels. As discussed in section 4, the emissivity/transmissivity effect is the sum of two physical processes of opposing sign: 1) the reduced longwave emissivity of the lower stratosphere due to ozone depletion, which acts to cool the troposphere; and 2) the increased transmissivity of the lower stratosphere to shortwave radiation, which acts to warm the troposphere. Therefore, the emissivity/transmissivity effect is negligible because it reflects two opposing processes that occupy a relatively small fraction of the atmospheric radiation spectrum. In contrast, the temperature effect accounts for the majority of the total simulated tropospheric temperature response because it has no offsetting shortwave heating term and encompasses longwave emission from a broader range of the atmospheric radiation spectrum.

b. Recent trends in the NH polar stratosphere

Results for trends in the NH polar stratosphere are displayed in Fig. 5. The top panel is a reproduction of the observations from Fig. 2 (left), and the bottom panel depicts the temperature effect of the stratospheric anomalies. As noted above, the emissivity/transmissivity effect of the stratospheric anomalies is negligible and hence is not shown for the NH trends. As in Fig. 3, the simulated temperatures are, by construction, identical to the observed temperatures above the tropopause (solid black line).

In general, the results for the NH trends are more difficult to interpret than those for the SH trends. The NH polar stratospheric temperature trends are much weaker than their SH counterparts, particularly in the lower stratosphere below 100 hPa. Consequently, the

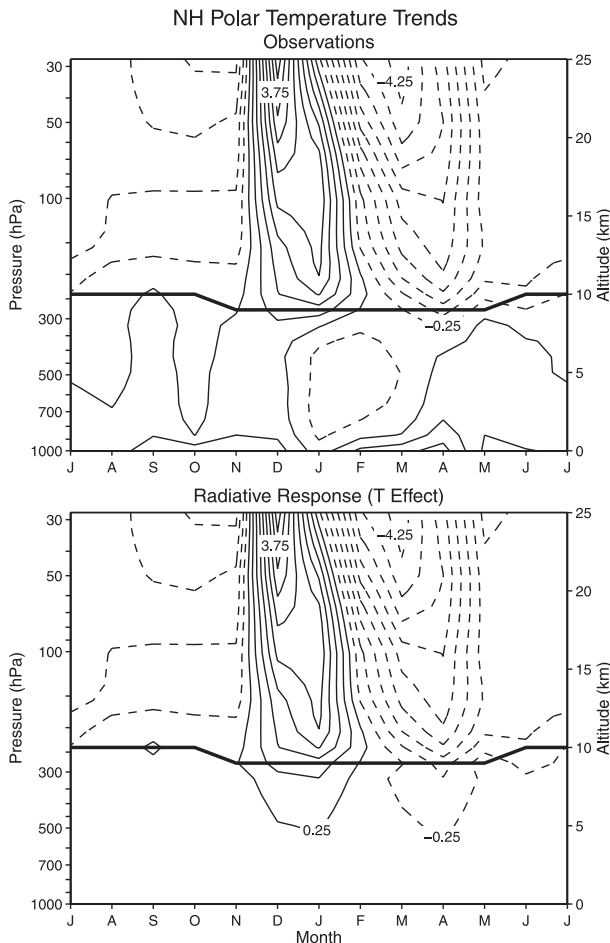


FIG. 5. (top) Reproduction of Fig. 2, left. (bottom) The radiative temperature response to NH polar stratospheric temperature forcing (the temperature effect). Positive contours are solid, and negative contours are dashed. The contour interval is 0.5 K ($-0.75, -0.25, 0.25, 0.75, \dots$). The region above the solid black line is used to set the stratospheric conditions for the radiative calculations.

NH polar tropospheric radiative temperature response is substantially smaller than that of the SH polar troposphere. The seasonality of the radiative temperature response also bears little resemblance to the observed changes in NH polar tropospheric temperatures: the radiative effects of the stratospheric temperature changes induce warming in the upper troposphere during December and January and cooling in the upper troposphere during March and April (Fig. 5, bottom), whereas the observations are dominated by weak tropospheric cooling during January and February (Fig. 5, top).

The results in Fig. 5 suggest that the anomalous radiative heating rates associated with NH polar stratospheric climate change only weakly perturb the temperature field of the NH polar troposphere. The results also reveal that physical processes other than the radiative effects of

stratospheric temperature and ozone anomalies must play a dominant role in determining the changes in NH polar tropospheric temperatures observed over the period 1979–2001.

6. Conclusions

The purpose of this study is to assess the radiative temperature response of the polar troposphere to stratospheric variability. The radiative response of the troposphere is quantified for both SH and NH polar stratospheric climate trends. In each case, the net radiative response is dominated by the changes in stratospheric temperatures; the net response due to changes in stratospheric emissivity and transmissivity caused by ozone is negligible.

In the case of the SH stratospheric trends, the mid- and upper tropospheric radiatively induced temperature response bears strong resemblance to the observed temperature trends during late austral spring and early austral summer. As in the observations, the upper-tropospheric radiative response exceeds 1 K in December. The radiative response does not capture the observed cooling near the surface during early austral summer, likely because the radiative calculations do not account for changes in surface radiative absorption or atmospheric dynamics.

The results for the NH stratospheric trends are more difficult to interpret. The NH stratospheric trends are much smaller than their SH counterparts, and hence the radiative temperature response of the NH polar troposphere is weaker than that of the SH polar troposphere. The weak calculated changes in NH polar tropospheric temperatures also bear little resemblance to the observed changes there. The results thus imply that the NH polar tropospheric temperature trends are not strongly affected by the radiative impacts of NH polar stratospheric climate trends.

Overall, our primary conclusion is that the anomalous radiative heating rates associated with large polar lower-stratospheric temperature anomalies have a demonstrable impact on polar tropospheric temperatures. However, our approach has two obvious caveats. First, the calculations neglect the role of tropospheric dynamics. The omission of tropospheric dynamics is by design, as we wish to isolate and quantify the role of radiative processes in stratosphere–troposphere coupling. But it is worth emphasizing that the agreement between the observations and the radiative calculations does not diminish the importance of tropospheric dynamics; rather, the agreement reveals that tropospheric dynamics need not be invoked to explain the observed changes in SH polar tropospheric temperatures. The second caveat is that our calculations neglect changes in

tropospheric water vapor. The longwave radiative impact of water vapor is approximately proportional to changes in the logarithm of its concentration (e.g., Raval and Ramanathan 1989). Therefore, even though temperatures are cold in the polar regions, water vapor may still play a nontrivial role in determining the net tropospheric temperature response to a stratospheric radiative anomaly. Unfortunately, the variability and trends in water vapor in these regions are poorly constrained by observations. Furthermore, it is unclear how relative humidity and hence water vapor concentrations are affected by temperatures changing locally over the polar cap. For these reasons, we do not consider the effects of tropospheric water vapor in our calculations.

The radiative effect of the lower-stratospheric temperature anomalies revealed here provides a simple mechanism whereby “information” about the stratospheric flow is communicated to tropospheric levels. It remains to be determined to what extent the radiatively induced changes in tropospheric temperatures, in turn, trigger the observed changes in tropospheric eddy activity. It would be interesting to assess the importance of radiative processes in this regard by forcing a general circulation model with the tropospheric heating rates calculated here.

Acknowledgments. We thank Susan Solomon and three anonymous reviewers for their helpful comments and suggestions. KMG was supported in part by a National Science Foundation Graduate Research Fellowship, and both KMG and DWJT were supported by National Science Foundation Grant ATM-0613082.

REFERENCES

- Arblaster, J. M., and G. A. Meehl, 2006: Contributions of external forcings to southern annular mode trends. *J. Climate*, **19**, 2896–2905.
- Baldwin, M. P., and T. J. Dunkerton, 1999: Propagation of the Arctic Oscillation from the stratosphere to the troposphere. *J. Geophys. Res.*, **104**, 30 937–30 946.
- , and —, 2001: Stratospheric harbingers of anomalous weather regimes. *Science*, **294**, 581–584.
- Chen, G., I. M. Held, and W. A. Robinson, 2007: Sensitivity of the latitude of the surface westerlies to surface friction. *J. Atmos. Sci.*, **64**, 2899–2915.
- Fels, S. B., J. D. Mahlman, M. D. Schwarzkopf, and R. W. Sinclair, 1980: Stratospheric sensitivity to perturbations in ozone and carbon dioxide: Radiative and dynamical response. *J. Atmos. Sci.*, **37**, 2265–2297.
- Forster, P. M. de F., and K. P. Shine, 1997: Radiative forcing and temperature trends from stratospheric ozone changes. *J. Geophys. Res.*, **102**, 10 841–10 855.
- , and —, 2002: Assessing the climate impact of trends in stratospheric water vapor. *Geophys. Res. Lett.*, **29**, 1086, doi:10.1029/2001GL013909.

- , R. S. Freckleton, and K. P. Shine, 1997: On aspects of the concept of radiative forcing. *Climate Dyn.*, **13**, 547–560.
- Gillett, N. P., and D. W. J. Thompson, 2003: Simulation of recent Southern Hemisphere climate change. *Science*, **302**, 273–275.
- Haynes, P. H., C. J. Marks, M. E. McIntyre, T. G. Shepherd, and K. P. Shine, 1991: On the “downward control” of extratropical diabatic circulations by eddy-induced mean zonal forces. *J. Atmos. Sci.*, **48**, 651–678.
- Kalnay, E., and Coauthors, 1996: The NCEP/NCAR 40-Year Reanalysis Project. *Bull. Amer. Meteor. Soc.*, **77**, 437–471.
- Kistler, R., and Coauthors, 2001: The NCEP–NCAR 50-Year Reanalysis: Monthly means CD-ROM and documentation. *Bull. Amer. Meteor. Soc.*, **82**, 247–267.
- Kushner, P. J., and L. M. Polvani, 2004: Stratosphere–troposphere coupling in a relatively simple AGCM: The role of eddies. *J. Climate*, **17**, 629–639.
- Langematz, U., M. Kunze, K. Krüger, K. Labitzke, and G. L. Roff, 2003: Thermal and dynamical changes of the stratosphere since 1979 and their link to ozone and CO₂ changes. *J. Geophys. Res.*, **108**, 4027, doi:10.1029/2002JD002069.
- Limpasuvan, V., D. W. J. Thompson, and D. L. Hartmann, 2004: The life cycle of the Northern Hemisphere sudden stratospheric warmings. *J. Climate*, **17**, 2584–2596.
- Manney, G. L., K. Krüger, J. L. Sabutis, S. A. Sena, and S. Pawson, 2005: The remarkable 2003–2004 winter and other recent warm winters in the Arctic stratosphere since the late 1990s. *J. Geophys. Res.*, **110**, D04107, doi:10.1029/2004JD005367.
- Newman, P. A., and Coauthors, 2003: Polar stratospheric ozone: Past and future. *Scientific Assessment of Ozone Depletion: 2002*, Global Ozone Research and Monitoring Project Rep. 47, World Meteorological Organization, 3.1–3.104.
- , and Coauthors, 2007: Polar ozone: Past and present. *Scientific Assessment of Ozone Depletion: 2006*, Global Ozone Research and Monitoring Project Rep. 50, World Meteorological Organization, 4.1–4.48.
- Polvani, L. M., and P. J. Kushner, 2002: Tropospheric response to stratospheric perturbations in a relatively simple general circulation model. *Geophys. Res. Lett.*, **29**, 1114, doi:10.1029/2001GL014284.
- Ramanathan, V., 1977: Troposphere–stratosphere feedback mechanism: Stratospheric warming and its effect on the polar energy budget and the tropospheric circulation. *J. Atmos. Sci.*, **34**, 439–447.
- , and R. E. Dickinson, 1979: The role of stratospheric ozone in the zonal and seasonal radiative energy balance of the earth–troposphere system. *J. Atmos. Sci.*, **36**, 1084–1104.
- Randel, W. J., and F. Wu, 1999: Cooling of the Arctic and Antarctic polar stratospheres due to ozone depletion. *J. Climate*, **12**, 1467–1479.
- , and —, 2007: A stratospheric ozone profile data set for 1979–2005: Variability, trends, and comparisons with column ozone data. *J. Geophys. Res.*, **112**, D06313, doi:10.1029/2006JD007339.
- , —, and R. Stolarski, 2002: Changes in column ozone correlated with the stratospheric EP flux. *J. Meteor. Soc. Japan*, **80**, 849–862.
- , and Coauthors, 2009: An update of observed stratospheric temperature trends. *J. Geophys. Res.*, **114**, D02107, doi:10.1029/2008JD010421.
- Raval, A., and V. Ramanathan, 1989: Observational determination of the greenhouse effect. *Nature*, **342**, 758–761.
- Reed, R. J., J. L. Wolfe, and H. Nishimoto, 1963: A spectral analysis of the energetics of the stratospheric sudden warming of early 1957. *J. Atmos. Sci.*, **20**, 256–275.
- Shine, K. P., and Coauthors, 2003: A comparison of model-simulated trends in stratospheric temperatures. *Quart. J. Roy. Meteor. Soc.*, **129**, 1565–1588.
- Solomon, S., R. W. Portmann, T. Sasaki, D. J. Hofmann, and D. W. J. Thompson, 2005: Four decades of ozonesonde measurements over Antarctica. *J. Geophys. Res.*, **110**, D21311, doi:10.1029/2005JD005917.
- , —, and D. W. J. Thompson, 2007: Contrasts between Antarctic and Arctic ozone depletion. *Proc. Natl. Acad. Sci. USA*, **104**, 445–449.
- Song, Y., and W. A. Robinson, 2004: Dynamical mechanisms for stratospheric influences on the troposphere. *J. Atmos. Sci.*, **61**, 1711–1725.
- Thompson, D. W. J., and S. Solomon, 2002: Interpretation of recent Southern Hemisphere climate change. *Science*, **296**, 895–899.
- , and —, 2005: Recent stratospheric climate trends as evidenced in radiosonde data: Global structure and tropospheric linkages. *J. Climate*, **18**, 4785–4795.
- , M. P. Baldwin, and S. Solomon, 2005: Stratosphere–troposphere coupling in the Southern Hemisphere. *J. Atmos. Sci.*, **62**, 708–715.
- , J. C. Furtado, and T. G. Shepherd, 2006: On the tropospheric response to anomalous stratospheric wave drag and radiative heating. *J. Atmos. Sci.*, **63**, 2616–2629.
- Wittman, M. A. H., A. J. Charlton, and L. M. Polvani, 2007: The effect of lower stratospheric shear on baroclinic instability. *J. Atmos. Sci.*, **64**, 479–496.